

# Investigative Study of Corrosion Inhibition of *Newbouldia leavis* Extracts on Mild Steel in 1M NaOH and KOH Solutions

J. J. O. Ajali<sup>1\*</sup>, V.E. Ojukwu<sup>2</sup>, O. E. Achugbu<sup>3</sup>, C. C. Ejiofor<sup>4</sup>, C. N. Onyenanu<sup>5</sup>, L.N. Emembolu<sup>6</sup>, J.T. Nwabanne<sup>7</sup>  
<sup>1,2,3,4,5,6,7</sup>Department of Chemical Engineering, Nnamdi Azikiwe University, Awka  
ORCID ID: <https://orcid.org/0009-0003-6685-3081>

**Abstract:-** The corrosion inhibition of *Newbouldia leavis* (NL) leaf extract on mild steel in alkaline media was investigated in this study. The plant leaf extract's functional groups comprise of oxygen and nitrogen atoms (O-H, N-H, C-N, C-O, C=O, and CN) as well as aromatic rings, according to FTIR data. Phytochemical analysis showed the presence of tannins, saponins, phytates, phenolics, flavonoids, cardiac glycosides and alkaloids. The results also showed that mild steel exhibits a considerable shift to passivation within the examined potential range. The inhibitors' molecules created an excellent protective coating on the mild steel, according to SEM micrographs. Adsorption of plant extracts on metal surfaces was spontaneous and occurred via the physical adsorption process. The measurements of gravimetric, thermometric, potentiodynamic polarization and electrochemical impedance spectroscopy results showed that the inhibition efficiency rose with increasing concentration of inhibitors and decreased with increasing temperature. The findings of the potentiodynamic polarization indicated that the plant leaf extracts were mixed-type inhibitors because  $E_{corr}$  value greater than 85mV confirms that the NL extract is a mixed-type inhibitor. The findings of electrochemical impedance spectroscopy demonstrated that adding inhibitors enhanced the charge-transfer resistance of the corrosion process and hence the inhibition performance. The inhibition efficiency (IE%) in the presence of 200mg/l and 1000mg/l of NL inhibitor was gotten to be 71.2% and 87.9% respectively for 1M KOH medium and 95.6% and 97.1% respectively for 1M NaOH medium. Quantum chemical parameters indicated that the inhibitor molecules' active ingredients slowed the corrosion of mild steel as was confirmed by density functional theory.

**Keyword:-** Alkaline corrosion, electrochemical impedance spectroscopy, Density Functional Theory (DFT), potentiodynamic polarization or quantum chemical calculations.

## I. INTRODUCTION

Metals or their alloys deteriorate via reactions when they are subjected to extreme conditions in the environment [1]. An increase in industrial activities has led to new dimensions of corrosion problems and has necessitated research into the protection of metals like mild steel [2]. Mild steel is a choice metal in many engineering applications, constructions and other services because of the protective layer of oxide it forms when attacked [3], its

attractive mechanical properties [4] and its relatively affordable price [5]. The tendency for any material to corrode largely dependent on the metal's structural composition through the various formative steps, for instance, the alloying process [6]. In the same vein, in extreme or aggressive conditions such as acidic or alkaline media, they will be descaled, pickled [7], and have reduced ductility [8] hence deteriorating [9] with the impact ranging from mild to severe [10]. Generally, the impact of corrosion is felt gradually by the metallic material in form of operational complications [8]. Some factors like the Gibb's free energy play vital roles in the corrosion of metals as they initiate thermodynamic imbalance causing the metal to return to its natural oxide state and thereby corrode in the process.

Also the methods used to deal with corrosion include coatings, cathodic protection and the use of inhibitors [11]. Among the many methods of dealing with the problem of corrosion, the most common technique is corrosion inhibition since it is efficient and simple to use [12]. Inhibitors of corrosion are used to slow down the pace of corrosion [13] or to effectively retard the process [14] by preventing the formation of chloride ions or a more resistant oxide film [4] with the aid of surfactants molecules which are good for surface and interface interactions [15]. Inorganic inhibitors of choice are those of phosphate compounds namely; disodium hydrogen phosphate, disodium monofluoride phosphate, zinc phosphate and lithium zinc phosphate [14]. Compounds with functional electronegative groups or electrons in triple or conjugated double bonds are the best inhibitors [7] for instance pigment in paint coating [8], expired drugs [16] and chemical medicines [17] like quinoxaline and pyrazine [18]. Despite their effectiveness, inorganic inhibitors are toxic and constitute a danger to our environment [10] and are highly recalcitrant and persistent due to the presence of chromates and phosphates [5]. Synthesized inhibitors are good in corrosion prevention, however, their usage has been greatly marred by their toxicity to living organisms and the environment [19] and their high cost of manufacture [5].

In pursuance of the green revolution and by way of achieving sustainable development goals, affordable [20] non-toxic, biodegradable and environmentally sustainable [2] and friendly inhibitors are used [6]. These biomasses are natural, cheap and readily available plant leaf extracts containing biological components known as phytochemicals [21] such as quinolones, quinoxaline [22], tannin, alkaloids and nitrogen bases, carbohydrates, amino acids and proteins

[23]. The natural plant leaf extracts are suitable for application in corrosion inhibition and are equally affordable, readily available and renewable. Generally, these plant extracts form protective coating on metal surface which will inhibit the corrosion process [24]. The efficiency depends on the structure and make-up of the adsorbed layer. Organic inhibitors create chelates on metal surfaces by transferring electrons from the inhibitor to the metal surface due to lone pair and Pi-electron [4]. In addition, steel passivation in alkaline environment can be attributed to the development of an extremely thin yet highly protective oxide/hydroxide layer containing nitrogen and sulphur atoms [25, 26] by displacing water molecule to form compact barrier film [23]. This is strengthened by the HOMO and LUMO (the highest occupied molecular orbital and lowest empty molecular orbital) (the geometry of the inhibitor molecules at their ground state and the nature of their molecular orbitals) [22]. Using response surface methodology (CCD) modelling, Emembolu, Onukwuli [13] achieved an inhibitory efficiency of 82.93% under the ideal conditions of 0.055g/l acid concentration, 333k temperature, and 2.75h immersion time. Chaudhari and Vashi [1] investigated the Henna leaves' inhibitory effect on mild steel in an acetic acid medium. It was found that corrosion rate increased with concentration of acid while the corrosion inhibition increased as concentration of leave extract increased. This present work aims investigating the inhibition efficiency of *Newbouldialeavis* on mild steel in KOH and NaOH medium by measurement of the electrochemical impedance spectroscopy, potentiodynamic polarization and quantum chemical studies.

## II. EXPERIMENTAL

### A. Material collection and preparation

The *Newbouldialeavis* leaf and other materials used in this research work were locally sourced from Awka in Anambra state of Nigeria. All chemicals and reagents used are of analytical quality and do not require further purification. Mild steel samples containing P (0.02%), Mn (0.11%), Si(0.02%), S(0.02%), Cu(0.01%), C (0.23%), Ni (0.02), Cr (0.01%), and Fe (99.56%) were mechanically cut into pieces of 5 cm x 4 cm in size with a thickness of 0.1 cm. The mild steel pieces were cleaned and polished with emery cloths of varied grades (200, 400, 600, 800 and 1000) to expose the shiny polished surface. Oil and organic impurities were removed using acetone and subsequently washed with distilled water, dried and stored in a desiccator. For accuracy, the weights of the mild steel pieces were obtained in triplicates and labelled systematically.

### B. Extraction of *Newbouldialeavis* Extract (Inhibitor)

New *bouldialeavis* (NL) samples collected were identified at Faculty of Biosciences, NnamdiAzikiwe University, Awka. NL leaves weighing 40g were washed in distilled water and dried for two days at room temperature. The leaves were subsequently reduced to powder in order to maximize their surface area, and then they were submerged in 500ml of ethanol in a beaker and covered for 48 hours. The mixture was filtered to remove the solid particles and the ethanol- extract solution gotten. The extract (inhibitor) in

the solution was concentrated by evaporating the ethanol through heating. The solution was made in various concentrations of 1M NaOH and KOH with inhibitor concentrations of 200mg/l and 1000mg/l.

### C. Characterization Studies

Instrumental characterization of *Newbouldialeavis* leaf extracts was performed using Fourier transform infrared spectroscopy (FTIR) and Scanning Electron Microscope (SEM). FTIR analysis was carried out before and after the corrosion process to determine the functional groups present in the extract before and after the process and the ones left on the inhibited medium (the corrosion products). While the scanning electron microscope was used to analyse the surface structure of the mild steel coupons in the uninhibited and inhibited mediums before and after the corrosion process respectively. Phytochemical analysis was run on the *Newbouldialeavis* leaf extract using the method specified by Emembolu and Onukwuli [24]. This was done to determine the presence of tannin, saponin, polyphenols, flavonoids, alkaloids, cardiac glycosides and quinolones [27, 28]

### D. Electrochemical Studies

Mild steel coupons were cut and prepared for the electrochemical experiment so that just 1 cm was left exposed enabling simple removal of the coupons at the conclusion of each experimental run. The electrodes were degreased by ethanol, rinsed with distilled water, polished with emery sheets ranging from 600 to 1000, and dried in acetone. Utilizing a corrosion system and VERSASTAT 300 complete dc voltmeter together with V3 studio software for electrochemical impedance spectroscopy, electrochemical experiments were carried out in a three-electrode corrosion cell. A mild steel sample, known as the working electrode, a platinum electrode, known as the auxiliary electrode, and a reference electrode (a saturated calomel electrode), are the three electrodes. 20mL of electrolyte were utilized in the corrosion setup. In a water bath with a constant temperature, the corrosion was examined. This improves temperature regulation. Then, potentiodynamic polarization tests were performed using a potentiodynamic/Galvanostat corrosion system and E-chem software. A saturated calomel electrode (SCE) was employed as the reference electrode and a graphite rod served as the counter electrode [23]. They were connected by a lugging capillary. At the end of the 1800s, impedance measurements were made in aerated and unstirred solutions at a temperature of 30°C. With a signal amplitude perturbation of 5 mV, impedance measurements were conducted at corrosion potentials ( $E_{corr}$ ) spanning the frequency range of 100 KHz-0.1 Hz. Using Nyquist plots and the inhibition efficiency (IE%) for various inhibitor doses.

$$IE\% = \left( \frac{R_{ct(inh)} - R_{ct}}{R_{ct(inh)}} \right) \times 100 \quad (1)$$

Where  $R_{ct}$  and  $R_{ct(inh)}$  denote charge transfer resistance in the absence and presence of inhibitor.

**E. Potentiodynamic polarization**

Potentiodynamic polarization tests were conducted for mild steel between -250 and +400 mV and in the potential range of 250 mV vs corrosion potential at a scan rate of 0.333 mVs-1. To ensure that the data could be reproduced, each test was carried out three times. At a temperature of 30°C, all experiments were conducted in freshly produced solutions. Equation (2) was used to determine the inhibition efficiency.

$$IE\% = \frac{i_{corr( uninhib )} - i_{corr( inh )}}{i_{corr( uninhib )}} \times 100 \tag{2}$$

Where  $i_{corr( uninhib )}$  and  $i_{corr( inh )}$  are the corrosion current density values without and with inhibitors, respectively.

**III. RESULTS AND DISCUSSIONS**

**A. Characterization Results**

➤ **FTIR results**

FTIR results revealed that the plant leaf extracts contain oxygen and nitrogen atoms (O–H, N–H, C–N, C–O, C=O and C≡N) and aromatic rings in their functional groups. There were reductions in peaks of the functional groups of the corrosion products compared to the peaks of the pure leaf extracts from FTIR analysis. Table 1.0 presents the analysis of pure *Newbouldialeavis* leave extract and scratched mild steel oxide film. O-H stretches showed peaks of 3675.66cmol2/kJ2 shifted to O-H stretch (3329.04 cmol2/kJ2); C-H stretch (2761.99-3119.74 cmol2/kJ2) shifted to C-H stretch 3174.74 cmol2/kJ2 and C=C, C≡N stretches shifted to 2187.22 C≡C, C≡N aromatic stretches, N-O (1435.09 cmol2/kJ2) asymmetric stretch shifted to N=O (1292.28 cmol2/kJ2) symmetric stretch. C-H bend in the plane (1003.77 cmol2/kJ2) shifted to 921.96 cmol2/kJ2. C=H-H, Ar-H bend out of the plane. The adsorption operation in this analysis indicated that the extracts were adsorbed on the surface of the metal.

Table 1: Peak, intensity and assignment of FTIR analysis of *New bouldialeavis* extract and scratched mild steel oxide film using KOH.

<i>Newbouldialeavis</i> leaves extract			scratched mild steel oxide film.		
Peak (cmol2/kJ2)	Intensity	Assignment	Peak (cmol2/kJ2)	Intensity	Assignment
1003.77	1.1243	C-H bend in the plane	921.96	2.6189	C=C-H, Ar-H bend out of the plane
1269.46	1.1964	C-O stretch	1168.84	3.3746	C-O stretch
			1261.42	2.8867	
1435.09	0.2010	N-O asymmetric stretch	1292.28	2.1001	N-O symmetric stretch
1619.13	2.7641	C=C stretch, C=N stretch	1600.88	2.617	C=C stretch, C=N stretch
2027.20	2.44843	C≡C stretch, C≡N stretch	2187.22	2.0436	C≡C stretch, C≡N stretch
			2310.66	2.5063	
2436.90	2.654	C≡C stretch, C≡N stretch	2156.36	2.6264	C≡C stretch, C≡N stretch
			2403.24	2.6979	
2761.99	1.4541	C-H stretch	2804.42	2.8647	C-H stretch
3119.74	1.7401	C-H stretch	3174.74	2.5713	C-H stretch
3675.66	5.5670	O-H stretch	3329.04	4.1986	O-H stretch

➤ **SEM results**

SEM images showed that the molecules of the inhibitors created a strong protective coating on the mild steel. The metal surfaces were clearly harmed by corrosion in the absence of the inhibitor, according to the electron micrographs, but the damage is far less in the presence of the inhibitor. This is related to the inhibitors' ability to effectively build a protective coating on the metal surfaces [29]. The findings of the weight loss strategy are closely correlated with the micrographs. This concurs with the

earlier research by Loto and Popoola [30]. The morphology of the MS surface in Fig. 1a shows that the surface was severely degraded in the absence of inhibitors, with patches of typical uniform corrosion. Even so, the rate of corrosion was slowed down in the presence of the green inhibitors in Fig. 1b because the inhibitor formed an adsorbed coating on the surface of the MS. The inhibitory efficiency evaluations made using the chemical and electrochemical methods reveal the protective character of the coating.

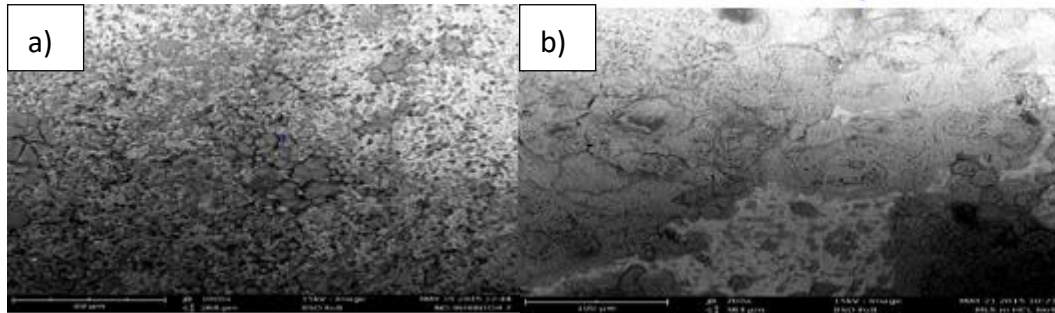


Fig 1: The micrograph of corroded mild steel surface in 1M KOH, (a) without *Newbouldialevis* leaf extract (b) with *Newbouldialevis* leaf extract.

**B. Phytochemical analysis results**

Phytochemical analysis showed the presence of tannins, saponins, phytates, phenolics, flavonoids, cardiac glycosides and alkaloids. The presence of these components indicates that the extract contains the active ingredients necessary for the corrosion inhibition process to occur.

**C. Potentiodynamic Polarization for MS**

The potentiodynamic polarization for MS in KOH and NaOH was evaluated in the absence and presence of *Newbouldialevis*. The results depicted in Fig. 2 are typical anodic and cathodic potentiodynamic polarization curves of mild steel in 1 M NaOH and 1 M KOH in the absence and presence of *Newbouldialevis*. It is obvious that both samples display significant transition to passivation within the potential range investigated. Considering the similarity

of the polarization curves for mild steel, one would expect a similar corrosion mechanism for both specimens. Based on the electrochemical parameters presented in Table 2, it is clear that the mild steel specimen was more susceptible to corrosive attack in the uninhibited environment compared to inhibited ones. This result is in line with [31]. The polarization curves indicate that the anodic dissolution reaction was predominantly affected compared to the cathodic reaction which was less perturbed, with similar results having been reported by [32]. The increased number of active sites could be responsible for the observed increase in the kinetics. The  $E_{corr}$  value greater than 85mV confirms that the NL extract is a mixed-type inhibitor as it recorded an  $E_{corr}$  value of 467 and 476 for 1M solution of NaOH and KOH, respectively [4].

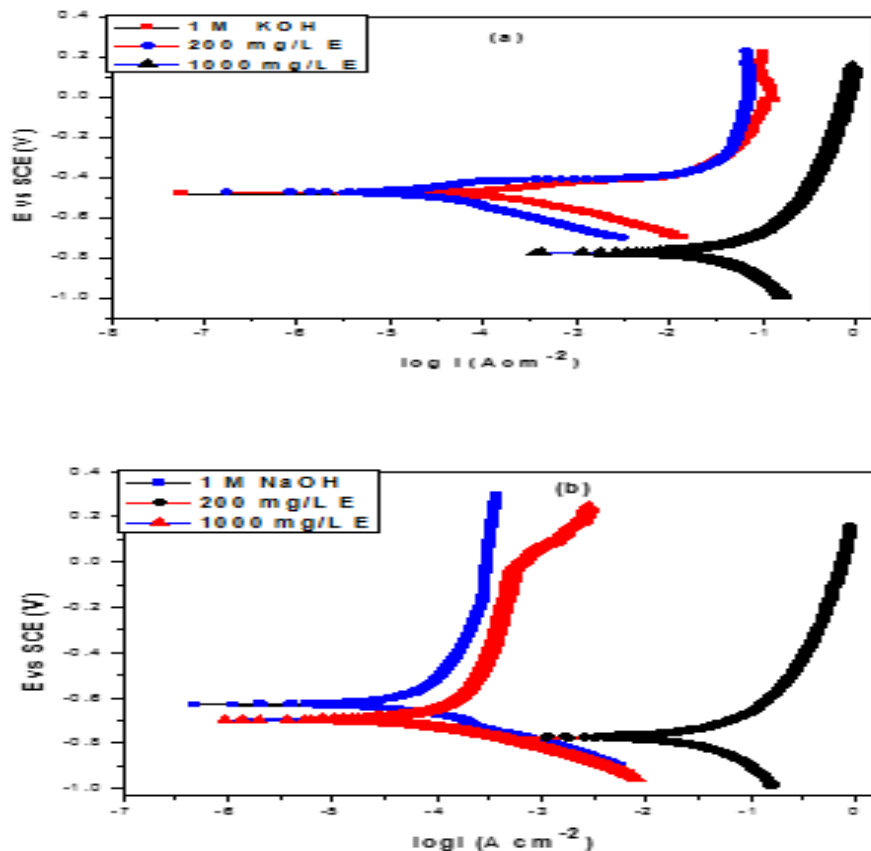


Fig. 2: Potentiodynamic polarization curves of mild steel in (a) 1M KOH and (b) 1MNaOH in the absence and presence of *Newbouldialevis*

Table 2: Polarization parameters for mild steel in 1M KOH and 1M NaOH in the absence and presence of various plant extracts

System	KOH			NaOH		
	$E_{corr}$ (mV/SCE)	$I_{corr}$ ( $\mu$ A/cm <sup>2</sup> )	IE%	$E_{corr}$ (mV/SCE)	$I_{corr}$ ( $\mu$ A/cm <sup>2</sup> )	IE%
<i>Newb.leavis</i>						
1M	- 529	196.2		-452	288.6	
200mg/L	- 536	57.6	70.6	-450	108.7	62.3
1000mg/L	- 476	24.1	87.7	-467	38.8	86.6

D. Electrochemical Impedance Spectroscopy (EIS)

Measurements for MS

In both the presence and absence of *Newbouldialeavis*, the electrochemical impedance spectroscopic (EIS) measurement of mild steel in NaOH and KOH solutions was investigated. The impedance spectra plots for mild steel in NaOH and KOH in the uninhibited and inhibited solutions are shown in Figs. 3 and 4. The relevant impedance parameters are listed in Table 3. The plots display a single depressed capacitive semicircle over the studied frequency range that is related to a single Bode Plot time constant. The interfacial charge transfer resistance ( $R_{ct}$ ) and the capacitive loop's diameter are both related to how charges are transferred across the metal/solution contact. Similarity between the graphs for mild steel in the two alkaline solutions suggests comparable corrosion mechanisms. However, the mild steel semicircle's smaller size in the unconstrained NaOH and KOH solutions suggests reduced charge transfer resistance, leading to a higher vulnerability to corrosion (Table 3). In both the presence and absence of NaOH and KOH, *Newbouldialeavis* hindered the corrosion response without altering the mechanism of the corrosion process in either system because its addition raised the impedance of mild steel in both solutions. The equivalent circuit model  $R_s$  ( $Q_{dl}R_{ct}$ ), which is often used to simulate the steel/acid interaction, was fitted to the impedance spectrum to investigate it. It is evident from the data in (Table 3) that  $R_{ct}$  for both systems rose as *Newbouldialeavis* concentration increased, indicating that

the electrode surfaces received more protection. The Helmholtz equation gives significant experimental evidence of inhibitor adsorption because the double-layer capacitance ( $C_{dl}$ ) for mild steel in both solutions decreased with an increase in inhibitor concentration. In other words, the adsorption of organic components of *Newbouldialeavis* (with lower dielectric constant than the displaced water molecules) on the metal/solution interface causes a decrease in the dielectric constant and/or an increase in the double layer thickness, which causes the lower  $C_{dl}$  values [4,33]. Therefore, greater  $R_{ct}$  values at higher *Newbouldialeavis* concentrations suggest improved extract adsorption on the mild steel surface, delaying the aggressive environment's attack during the corrosion reaction process [4, 33]. The variation in  $R_{ct}$  values provided a quantitative assessment of the protective impact. The values of achieved inhibitory efficacy are shown in Table 3. Due to the intrinsic changes in the features of each technique, there are very tiny differences in the computed inhibitory efficiency values from  $i_{corr}$  and  $R_{ct}$  values. For instance, the impedance measurements are performed (at  $E_{corr}$  and with minimum current transfer) on unaltered metal surfaces. In the presence of 200 mg/l and 1000 mg/l of the NL inhibitor, the inhibitory efficiency (IE%) was measured to be 71.2% and 87.9% for 1M KOH medium, respectively. While 200 mg/l and 1000 mg/l of NL inhibitor, respectively, resulted in 95.6% and 97.1% inhibition efficiency for 1M NaOH medium. This demonstrates that 1M NaOH or KOH had a greater inhibitory effect than 1M KOH.

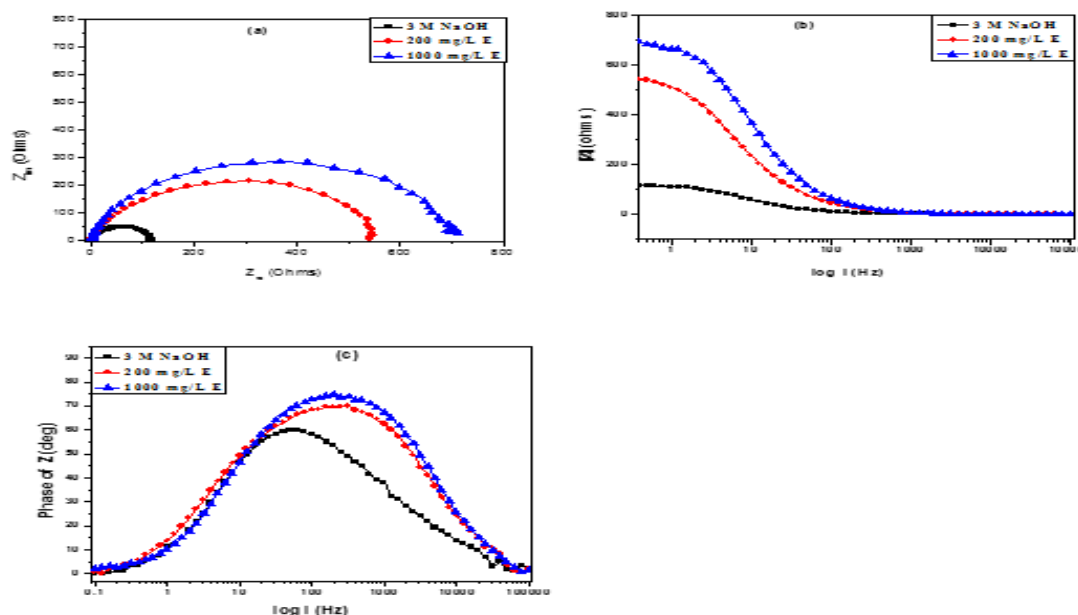


Fig. 3: Impedance spectra of mild steel in 1M NaOH solution in the absence and presence of *Newbouldialeavis*: (a) Nyquist, (b) Bode modulus and (c) Bode phase angle plots

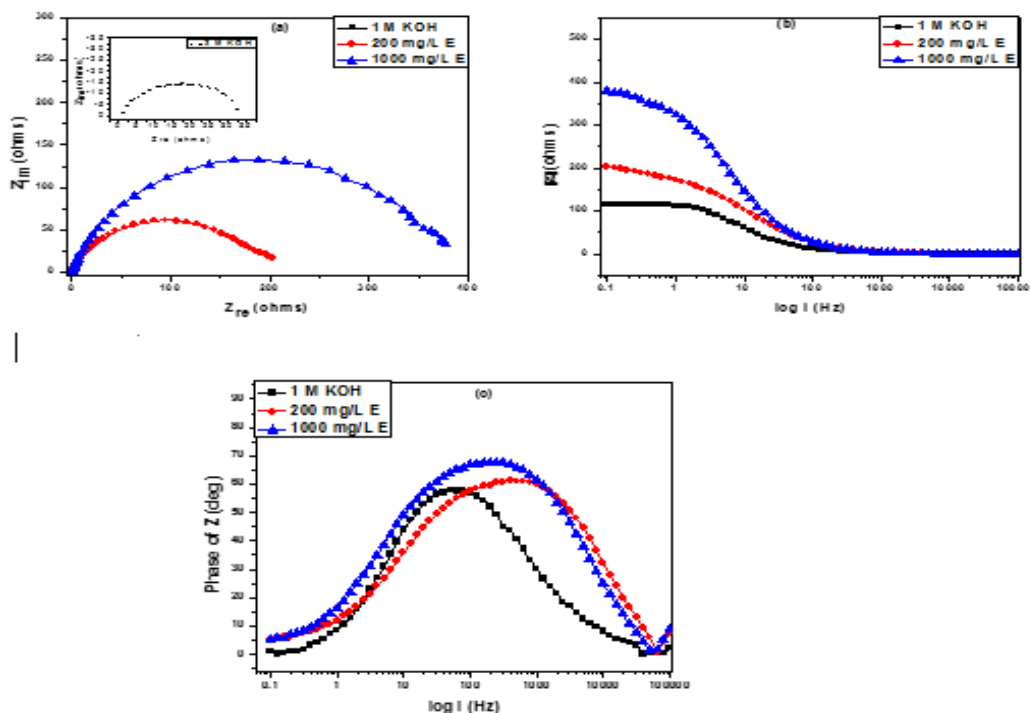


Fig. 4: Impedance spectra of mild steel in 1M KOH solution in the absence and presence of *Newbouldialeavis*: (a) Nyquist, (b) Bode phase angle and (c) Bode modulus.

Table 3: Electrochemical parameters for Mild steel in uninhibited and inhibited NaOH and KOH in *Newbouldialeavis*

System	$R_{LI}(\Omega\text{cm}^2)$	$R_s(\Omega\text{cm}^2)$	$R_{ct}(\Omega\text{cm}^2)$	$C_{dl}(\mu\text{F cm}^{-2})$	IE %
1 M KOH	6.2	2.13	98.7	3.12	
200 mg/L	412	3.23	400.2	1.54	71.2
1000 mg/L	1988	3.67	512.5	1.02	87.9
1 M NaOH	7.6	2.06	27.5	3.62	
200 mg/L	187	2.73	622	3.27	95.6
1000 mg/L	1124	3.33	932.3	2.99	97.1

E. Quantum Chemical Study for the mechanism of inhibition

It is clear from our first experimental findings that the corrosion-inhibiting properties of the active ingredients N-methyl-3,4methylenedioxy phenylpropan-3-amine (NMPA) of NL extracts are due to their adsorption on the mild steel surface. Density functional theory (DFT) has been used to precisely analyze data pertaining to molecular geometries and electron distributions and define the mechanism of inhibition by NL extracts, which has served to further corroborate our findings. Following geometric optimization for all nuclear coordinates, the parameters were generated. The adsorption centers in these molecules, which are in charge of interacting with the metal surface, may be accurately predicted using the frontier molecular orbital theory. The total electron density, the Fukui functions for electrophilic (F-) and nucleophilic (F+), and the highest occupied electrons are shown in Fig. 5(a) to (g).the lowest unoccupied molecular orbital (LUMO), which is the highest orbital in a molecule, and the highest orbital in a molecule. The heteroatoms found in the compounds under study predominately occupy the HOMO and LUMO energy orbitals. The adsorption centers of the inhibitors were estimated using the Mulliken charge analysis. The surface of

mild steel has a high capacity for adsorbing negatively charged atoms. The donor-acceptor interaction between inhibitor molecules and the metal surface is what causes the adsorption of inhibitor molecules on the metal surface. A flat-lying adsorption orientation was seen as a result of the electron density being delocalized all around the chosen molecules. The degree of surface coverage increases as a result of the increased contact caused by this orientation. However, the quantum chemical approach's calculated properties,The reactivity of these molecules can be determined from their estimated properties using a quantum chemical technique, but this reactivity cannot be directly transferred to the effectiveness of their ability to prevent corrosion, which requires additional processes such competitive adsorption, film formation, etc. As a result, optimizing the inhibitor structure was not possible using the correlations that were generated. Equation (3) was used to calculate the adsorption energy ( $E_{ads}$ ), which is crucial for describing the adsorption of these molecules onto the Fe surface.

$$E_{ads} = E_{total} - (E_{inhibitor} - E_{surface}) \tag{3}$$

$E_{\text{inhibitor}}$ ,  $E_{\text{surface}}$ , and  $E_{\text{total}}$  stand for the energy of a single molecule of these chosen active components, the energy of the Fe slab without adsorption, and the overall

energy of the system, respectively. The order of the calculated adsorption energy for the selected active constituents of the inhibitors is presented in Table 4.

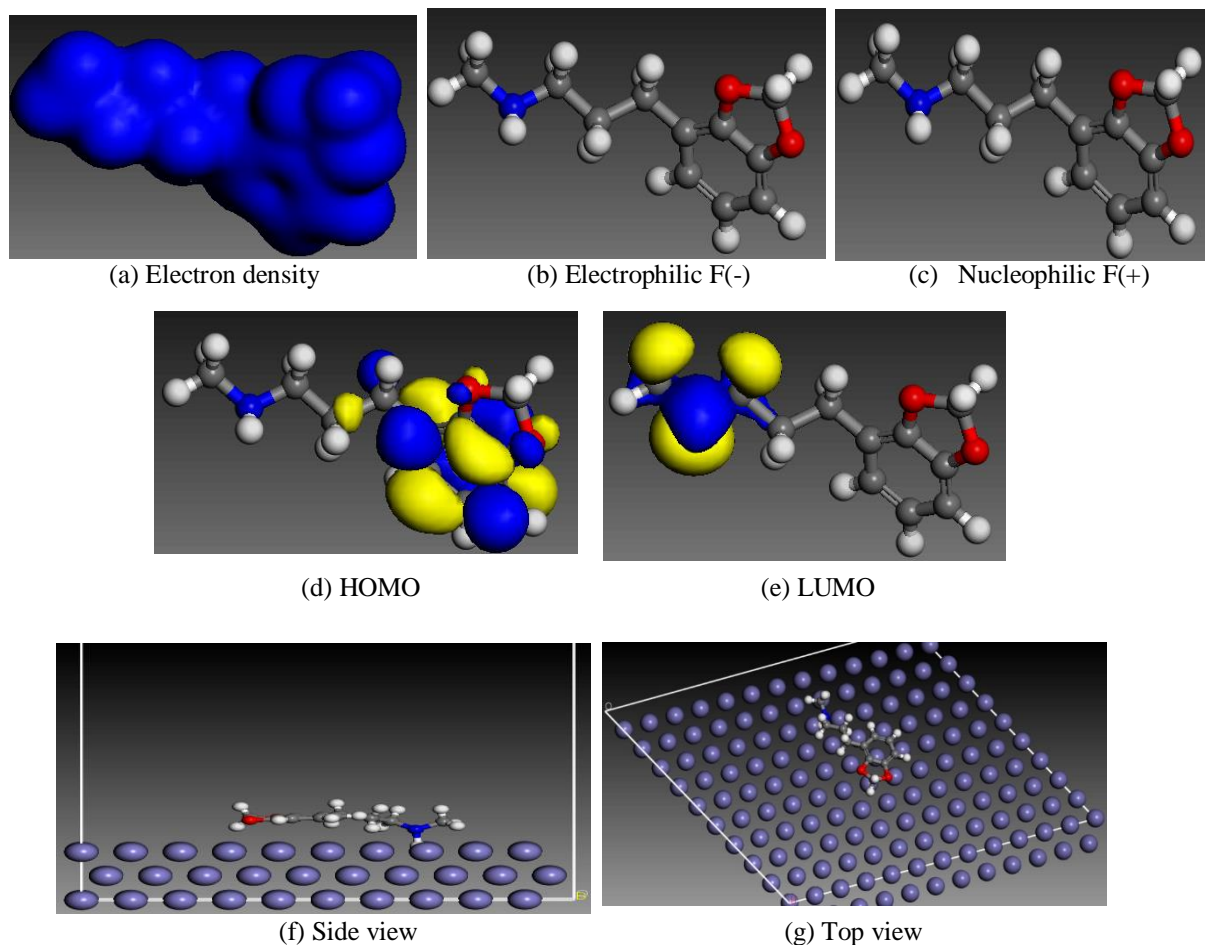


Fig. 4: Electronic properties of N-methyl-3,4-methylenedioxy phenylpropan-3-amine

- (a) Electron density, (b) electrophilic f (-), (c) nucleophilic f (+), (d) HOMO, (e) LUMO (f) side view of the snapshot for N-methyl-3,4-methylenedioxy phenylpropan-3-amine from molecular dynamics model. (g) top view of the Snapshot for N-methyl-3,4-methylenedioxy phenylpropan-3-amine from molecular dynamics model. **Atom legend:** white = H; grey = C; red = O. The blue and yellow isosurfaces depict the electron density difference: the blue regions show electron accumulation while the yellow regions show electron loss.

Table 4: Calculated quantum chemical properties for the most stable conformation of N-methyl-3,4-methylenedioxy phenylpropan-3-amine constituents of the NL extract

Molecule	$E_{\text{HOMO}}$ (eV)	$E_{\text{LUMO}}$ (eV)	$\Delta E$ (eV) (Kcal/mol)	Adsorption Energy (Å)	Molecular surface Area
NMPA	-5.363	-1.249	3.83	-53.6	252.1

#### IV. CONCLUSIONS

Corrosion inhibition of NL extract on mild steel in 1M NaOH and KOH solutions using different corrosion techniques was studied in this work. An increased number of sites upon exposure of mild steel to an alkaline solution led to an increase in the kinetics of both partial reactions via the formation of several electrochemical corrosion cells. A slight disparity noticed in the electrochemical impedance measurement of inhibition efficiency was due to the position of the metal surface used with a particular technique. In this paper, the research findings were validated using the Density Functional Theory (DTF) approach. This demonstrated that the delocalization of the electron density

all around the selected molecules is the cause of the accelerated kinetics of the metal-inhibitor interaction. As a result, higher  $R_{\text{ct}}$  values at higher NL extract concentrations demonstrate improved extract adsorption on the mild steel surface, which helps the surface resist the harsh environment's attack throughout the corrosion reaction process. The modest variations in the computed inhibitory efficiency values between the  $R_{\text{ct}}$  and  $i_{\text{corr}}$  values can be attributed to the inherent properties of each technique.

## REFERENCES

- [1.] Chaudhari, H. and Vashi, R. *The study of henna leaves extract as green corrosion inhibitor for mild steel in acetic acid*. Journal of Fundamental and Applied Sciences, 2016. **8**(2): p. 280-296.
- [2.] Akinbulumo, O.A., Odejebi, O. J. and Odekanle, E. L. *Thermodynamics and adsorption study of the corrosion inhibition of mild steel by Euphorbia heterophylla L. extract in 1.5 M HCl*. Results in Materials, 2020. **5**: p. 100074.
- [3.] Emembolu, L., Igbokwe, P. and Onyenanu, C. *Anticorrosion properties of Vitex doniana on Mild steel in HCl solution*. 2020. p. 3354-3362.
- [4.] Al-Amiery, A.A., Binti Kassim. Kadhum A. H. and Mohamad, B. *Synthesis and characterization of a novel eco-friendly corrosion inhibition for mild steel in 1 M hydrochloric acid*. Scientific reports, 2016. **6**(1): p. 1-13.
- [5.] Chigondo, M. and Chigondo, F. *Recent natural corrosion inhibitors for mild steel: an overview*. Journal of Chemistry, 2016. p 1-7.
- [6.] Ekeke, I. Nwanja, J. U., Nze, E. K. Udeze J. C. Okeke, H. E. and Herbert M. *Inhibitive Properties of Azadirachta Indica (Neem) Seed Extract on the Corrosion of Aluminum in 0.5 M Hcl Medium*. International Journal of Engineering Applied Science and Technology, 2020, vol. 4. issue 11, p. 45-49.
- [7.] Fiori-Bimbi, M.V., Gervasi, C., Alvarez P. E. and Vaca H. *Corrosion inhibition of mild steel in HCL solution by pectin*. Corrosion Science, 2015. **92**: p. 192-199.
- [8.] Oyekunle, D., Agboola, O. and Ayeni, A. *Corrosion inhibitors as building evidence for mild steel: a review*. in Journal of Physics: Conference Series. 2019. vol. 1378, Issue 3. 032046. IOP Publishing.
- [9.] Emembolu, L. N., Onukwuli O. D., Umembamalu, C. J. and Aniagor C. O. *Evaluation of the corrosion inhibitory effect of Napoleonaea Imperialis leaf extract on mild steel in a 1.3 M H2SO4 medium*. Journal of Bio-and Tribo-Corrosion, 2020. **6**(4): p. 1-15.
- [10.] Loto, C. A. and Loto R. T. *Inhibition and Adsorption Effects of Lavandula and Ricinus Communis Oil on Mild Steel Corrosion in H2SO4*. Journal of Chemical Technology and Metallurgy, 2019. **54**(6): p. 1352-1360.
- [11.] Lin, B., Tang, J., Wang, Y., Wang, H. and Zuo, Y. *Study on synergistic corrosion inhibition effect between calcium lignosulfonate (CLS) and inorganic inhibitors on Q235 carbon steel in alkaline environment with Cl<sup>-</sup>*. Molecules, 2020. **25**(18): p. 4200.
- [12.] Gupta, R. K., Malviya, M., Verma C. and Quraishi M. A. *Aminoazobenzene and diaminoazobenzene functionalized graphene oxides as novel class of corrosion inhibitors for mild steel: experimental and DFT studies*. Materials Chemistry and Physics, 2017. **198**: p. 360-373.
- [13.] Emembolu, L., O. Onukwuli, and V. Okafor, *Characterization and Optimization study of Epiphyllum oxypetalum extract as corrosion inhibitor for mild steel in 3 M H2SO4 solutions*. World Scientific News, 2020. **145**: p. 256-273.
- [14.] Mohagheghi, A. and Arefinia, R. *Corrosion inhibition of carbon steel by dipotassium hydrogen phosphate in alkaline solutions with low chloride contamination*. Construction and Building Materials, 2018. **187**: p. 760-772.
- [15.] Fawzy, A., Ablthagafi, I. I. *Thermodynamic, kinetic and mechanistic approach to the corrosion inhibition of carbon steel by new synthesized amino acids-based surfactants as green inhibitors in neutral and alkaline aqueous media*. Journal of Molecular Liquids, 2018. **265**: p. 276-291.
- [16.] Palaniappan, N., Alphonsa J., Cole, I. S., Balasubramanian, K. and Bosco, I. G. *Rapid investigation expiry drug green corrosion inhibitor on mild steel in NaCl medium*. Materials Science and Engineering: B, 2019. **249**: p. 114423.
- [17.] Qiang, Y., Gup, L., Li, H. and Lan, X. *Fabrication of environmentally friendly Losartan potassium film for corrosion inhibition of mild steel in HCl medium*. Chemical Engineering Journal, 2021. **406**: p. 126863.
- [18.] Saranya, J., Sowmiya, M., Sounthari, P., Parameswari, K., Chitra, S. and Senthilkumar, K. *N-heterocycles as corrosion inhibitors for mild steel in acid medium*. Journal of Molecular Liquids, 2016. **216**: p. 42-52.
- [19.] Raghavendra, N. and Bhat, J. I. *Chemical components of mature areca nut husk extract as a potential corrosion inhibitor for mild steel and copper in both acid and alkali media*. Chemical engineering communications, 2018. **205**(2): p. 145-160.
- [20.] Nwosu, F. O., Owate, I. O. and Osarolube, E. *Acidic corrosion inhibition mechanism of aluminum alloy using green inhibitors*. Am. J. Mater. Sci, 2018. **8**: p. 45-50.
- [21.] Saxena, A., Prasad, D. and Haldhar, R. *Investigation of corrosion inhibition effect and adsorption activities of Cuscuta reflexa extract for mild steel in 0.5 M H2SO4*. Bioelectrochemistry, 2018. **124**: p. 156-164.
- [22.] Chaoui, A., Lgaz, H., Chung, I., Ali, I. H., Gaonkar, S. L., Subrahmanya, B. K., Salghi, R., Oudda, H., and Khan I. M. *Understanding corrosion inhibition of mild steel in acid medium by new benzonitriles: insights from experimental and computational studies*. Journal of Molecular Liquids, 2018. **266**(1): p. 603-616.
- [23.] Cang, H., Fei, Z., Shao, J., Shi, W. and Xu, Q. *Corrosion inhibition of mild steel by aloes extract in HCl solution medium*. International Journal of Electrochemical Science, 2013. **8**(1): p. 720-734.
- [24.] Emembolu, L.N. and O. Onukwuli, *Corrosion inhibitive efficacy of natural plant extracts on zinc in 0.5 M HCl solution*. The Pharmaceutical and Chemical Journal, 2019. **6**(2): p. 62-70.
- [25.] Berdimurodov, E., Kholikov, A., Akbarov, K., Guo, L., Abdullah, M. A. and Elik M. A. *Adsorption isotherm and SEM investigating of cucurbit [n] urils based corrosion inhibitors with gossypol for mild steel in alkaline media containing chloride ions*. in



- Advanced Engineering Forum*. 2017. Trans Tech Publ.
- [26.] Nnanna, L.A. and Nwadiuko O., Ekekwe, N. D., Ukpabi, C., Udensi, S., Okeoma, K., Onwuagba, B. N. and Mejeha, I. M. *Adsorption and inhibitive properties of leaf extract of Newbouldia leavis as a green inhibitor for aluminium alloy in H<sub>2</sub>SO<sub>4</sub>*. *Amer. J. Mater. Sci*, 2012. **1**(2): p. 143-148.
- [27.] Mayuri, P., *Screening of aianthus (Excelsa roxb.) for secondary metabolites*. *Journal of Current Pharmaceutical Research*, 2012. **10**(1): p. 19-219.
- [28.] Marcano, L. and Hasenawa, D. *Analysis of phytochemicals in leaves and seeds*. *Agronomy Journal*, 1991. **83**: p. 445-452.
- [29.] Shanthi, T. and Rajendran, S. *Corrosion resistance of mild simulate concrete pore solution in presence of carboxy methyl cellulose*. *Journal of Chemical, Biological and physical sciences*, 2013. **3**(4): p. 2550 - 2556.
- [30.] Loto, C.A. and Popoola, A. P. I. *Inhibition Effect of Dendrocalamus brandissi leaves extracts on aluminum in HCL, H<sub>3</sub>PO<sub>4</sub>, Solutions*. *Corrosion Science* 2012. **65**: p. 299 - 308.
- [31.] Husseien, M., Amer, A. A., El-Maghraby, A. and Hamedallah, N.A *comprehensive characterization of corn stalk and study of carbonized corn stalk in dye and gas oil sorption*. *Journal of Analytical and Applied Pyrolysis*, 2009. **86**(2): p. 360-363.
- [32.] Rethinnagiri, V., Jeyaprakash, P., Arunkumar, M., Maheswaran, V., and Madhiyalagan, A. *Investigation and inhibition of aluminum corrosion in hydrochloric acid solutions by organic compound*. *Advances in Applied Science Research*, 2012. **3**(3): p. 1718 - 1726.
- [33.] Al-Amiery, A. A., Mohamad, A. B., Kadhum, A. A. H., Shaker, L. M., Wan Isahak, W. S. and Takriff, M. S. *Experimental and theoretical study on the corrosion inhibition of mild steel by nonanedioic acid derivative in hydrochloric acid solution*. *Scientific Reports*. 2022, 12:4705.